STUDY OF STRANGENESS ENHANCEMENT IN LEAD-LEAD COLLISIONS AT THE CERN SPS

PRESENTED BY L. ŠÁNDOR FOR THE WA97 COLLABORATION:

E. Andersen[b], F. Antinori[e,k], N. Armenise[a], H. Bakke[b], J. Bán[g], D. Barberis[f], H. Beker[e], W. Beusch[e], I.J. Bloodworth[d], J. Böhm[m], R. Caliandro[a], M. Campbell[e], E. Cantatore[e], N. Carrer[k], M.G. Catanesi[a], E. Chesi[e], M. Dameri[f], G. Darbo[f], A. Diaczek[l], D. Di Bari[a], S. Di Liberto[n], B.C. Earl[d], D. Elia[a], D. Evans[d], K. Fanebust[b], R.A. Fini[a], J.C. Fontaine[i], J. Ftáčnik[g], B. Ghidini[a], G. Grella[o], M. Guida[o], E.H.M. Heijne[e], H. Helstrup[c], A.K. Holme[j], D. Huss[i], A. Jacholkowski[a], G.T. Jones[d], P. Jovanovic[d], A. Jusko[g], T. Kachelhoffer[p], J.B. Kinson[d], A. Kirk[d], W. Klempt[e], B.T.H. Knudsen[b], K. Knudson[e], I. Králik[g], V. Lenti[a], R. Lietava[e], R.A. Loconsole[a], G. Løvhøiden[j], M. Lupták[g], V. Mack[i], V. Manzari[a], P. Martinengo[e], M.A. Mazzoni[n], F. Meddi[n], A. Michalon[p], M.E. Michalon-Mentzer[p], P. Middelkamp[e], M. Morando[k], M.T. Muciaccia[a], E. Nappi[a], F. Navach[a], P.I. Norman[d], B. Osculati[f], B. Pastirčák[g], F. Pellegrini[k], K. Píška[m], F. Posa[a], E. Quercigh[e], R.A. Ricci[h], G. Romano[o], G. Rosa[n], L. Rossi[f], H. Rotscheidt[e], K. Šafařík[e], S. Saladino[a], C. Salvo[f], L. Šándor[g,e], G. Segato[k], M. Sené[l], R. Sené[l], S. Simone[a], W. Snoeys[e], P. Staroba[m], S. Szafran[l], M. Thompson[d], T.F. Thorsteinsen[c], G. Tomasicchio[a], G.D. Torrieri[d], T.S. Tveter[j], J. Urbán[g], M. Venables[d], O. Villalobos Baillie[d], T. Virgili[o], A. Volte[l], M.F. Votruba[d] and P. Závada[m].

[a] Dipartimento I.A. di Fisica dell'Università e del Politecnico di Bari and Sezione INFN, Bari, Italy
[b] Fysisk institutt, Universitetet i Bergen, Bergen, Norway
[c] Høgskolen i Bergen, Bergen, Norway
[d] School of Physics and Astronomy, University of Birmingham, Birmingham, UK
[e] CERN, European Laboratory for Particle Physics, Geneva, Switzerland
[f] Dipartimento di Fisica dell'Università and Sezione INFN, Genoa, Italy
[g] Institute of Experimental Physics, Slovak Academy of Sciences, Košice, Slovakia
[h] INFN, Laboratori Nazionali di Legnaro, Legnaro, Italy
[i] GRPHE, Université de Haute Alsace, Mulhouse, France
[j] Fysisk institutt, Universitetet i Oslo, Oslo, Norway
[k] Dipartimento di Fisica dell'Università and Sezione INFN, Padua, Italy
[l] Collège de France and IN2P3, Paris, France
[m] Institute of Physics, Academy of Sciences of the Czech Republic, Prague, Czech Republic
[n] Dipartimento di Fisica dell'Università "La Sapienza" and Sezione INFN, Rome,Italy
[o] Dipartimento di Scienze Fisiche "E.R. Caianiello" dell'Università and INFN, Salerno, Italy
[p] Institut de Recherches Subatomiques, IN2P3/ULP, Strasbourg, France

A review of the latest results from the WA97 experiment on the strange particle production in Pb–Pb and p–Pb collisions is presented. Transverse mass spectra and yields of K^0_S, Λ, Ξ, Ω and h^- (negatively charged particles) have been measured at central rapidity. Yields are studied as a function of the number of nucleons participating in the collision N_{part}. From p–Pb to Pb–Pb collisions the particle yields per participant increase substantially. The enhancement is more pronounced for multistrange particles, and exceeds an order of magnitude for Ω.

1 Introduction

Strange particles, produced in high-energy heavy-ion collisions, are amongst the most powerful tools for the study of reaction dynamics. What makes this field of research particularly challenging is the prediction that the yield of strange, and especially multiply-strange, (anti-) particles should be strongly enhanced in the presence of a quark-gluon plasma (QGP) as compared to a purely hadronic scenario at the same temperature [1,2]. The strangeness enhancement, as well as the quarkonium suppression, is recognised as a sensitive probe of deconfinenent in the search for a QGP (see, e.g., recent reviews [3,4]).

Strangeness enhancement in heavy ion collisions was observed in several experiments performed at the CERN SPS and AGS [5]. The state of the art in the strange sector of ultra-relativistic heavy-ion collisions is regularly discussed in a series of topical conferences on the strangeness in quark matter, the last of which was held in July 1998 at Padova. The survey of results available from experiments at the CERN SPS prior to the Padova meeting can be found in [6].

Three heavy-ion experiments (WA85, WA94 and WA97) performed at the CERN Omega facility concentrated on high-statistics studies of strange and multiply-strange particles at mid-rapidity. The WA85 and WA94 experiments utilised the 200 A GeV/c SPS sulphur beam. WA85 investigated strangeness production in S–W and p–W collisions, whereas WA94 studied S–S and p–S interactions. Both experiments showed evidence for enhanced production of Λ ($|S| = 1$) and Ξ ($|S| = 2$) in nucleus-nucleus with respect to proton-nucleus collisions [7,8]. The WA97 experiment has extended this study to the heavier Pb–Pb system using the 158 A GeV/c SPS lead beam and has permitted the measurement of the rare Ω ($|S| = 3$) signal.

At present WA97 is finalising the first stage of its data analysis. A comprehensive picture of the strangeness production based on limited statistics is now available. Results on the hyperon production have been published [9,10]. The more complete results, with improved statistics of hyperons (by a factor of two) and new data on K^0_S and h^-, were presented at the Padova conference [11,12,13]. We shall concentrate on a review of these results.

2 Experimental procedure

2.1 The WA97 experiment

The WA97 experiment is designed to study strange particle production at central rapidity in Pb–Pb, p–Pb and p–Be collisions as a function of the strangeness content of the particles and of the number of nucleons taking part in the collisions. In order to cope with the increased track density in Pb–Pb collisions a new more powerful tracking detector - the silicon telescope - has been utilized. This ensured the capability of the experiment to perform an efficient pattern recognition, precise measurement of particle characteristics and reliable reconstruction of V^0 decays and multi-strange hyperon cascade decays. The experimental set-up, shown schematically in Fig. 1, is described in detail in ref. [14].

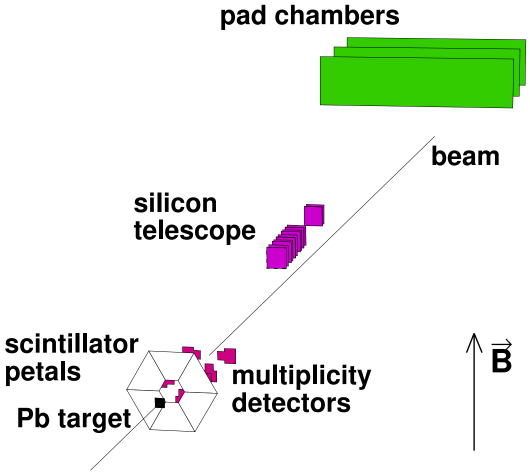

Figure 1. WA97 set-up. The target and all detectors (except for the pad chambers) are placed inside the homogeneous region of the 1.8 T Omega magnet.

The 158 A GeV/c lead beam from the CERN SPS was incident on a lead target with thickness corresponding to 1% of the interaction length. An 8% interaction length target was used for the p–Pb run. Scintillator petal detectors behind the target provided an interaction trigger selecting the most central ($\sim$ 40%) Pb–Pb collisions. Two planes of microstrip multiplicity detectors, covering the pseudorapidity region $2 \leq \eta \leq 3$ and $3 \leq \eta \leq 4$ respectively, provided information for detailed off-line study of the centrality dependence of particle ratios and spectra. In the proton reference runs at 158 GeV/c the protons were identified using Cherenkov CEDAR detectors [15], and a trigger was applied demanding at least two tracks in the telescope, as required to find V^0s.

The core of the WA97 set-up is a silicon telescope consisting of the novel pixel detectors [16] with a pixel size of 75×500 μm^2 and of silicon microstrip planes with a 50 μm pitch. The telescope (in the geometrical arrangement used in 1995 running) contained $\simeq 0.5 \times 10^6$ detecting elements and acted as a pixel tracking chamber (PTC). This precise tracking device was placed slightly above the beam line and inclined (pointing to the target) in order to accept particles at central rapidity and medium transverse momentum.

The reconstruction of tracks is done in the compact part of the PTC where silicon planes with surface of 5×5 cm^2 are closely packed over a distance of 30 cm. The momentum resolution of fast tracks is improved using the lever arm detectors which consisted of additional pixel and microstrip planes and of three MWPC's with a pad cathode readout.

The WA97 experimental set-up is symmetric with respect to the magnetic bending direction and, therefore, its geometrical acceptance is the same for particles and antiparticles.

2.2 Analysis of strange particle signals

The results presented here are based on the analysis of two data samples taken with lead (110 million events) and proton (120 million events) beams at 158 A GeV/c. The K^0_S and Λ, Ξ^-, Ω^- hyperons (and their antiparticles) were identified by reconstructing their decays into final states containing only charged particles:

$$\begin{array}{ll} K^0_S & \rightarrow \pi^+ + \pi^- \\ \Lambda & \rightarrow p + \pi^- \\ \Xi^- & \rightarrow \Lambda + \pi^- \\ & \quad \hookrightarrow p + \pi^- \\ \Omega^- & \rightarrow \Lambda + K^- \\ & \quad \hookrightarrow p + \pi^- \end{array}$$

We have analysed also a reference sample of negatively charged secondary particles. The details of the analysis, *i.e.* the extraction of the strange particle signals and the weighting for each reconstructed particle are discussed in [12,17]. In a given experimental arrangement there is no possibility to identify the secondary particles directly and, therefore, the extraction of the strange particle signals is performed using kinematic constraints. Fig. 2 demonstrates the excellent capability of the experiment to separate Ξ and Ω signals in the high track density environment of central Pb–Pb collisions.

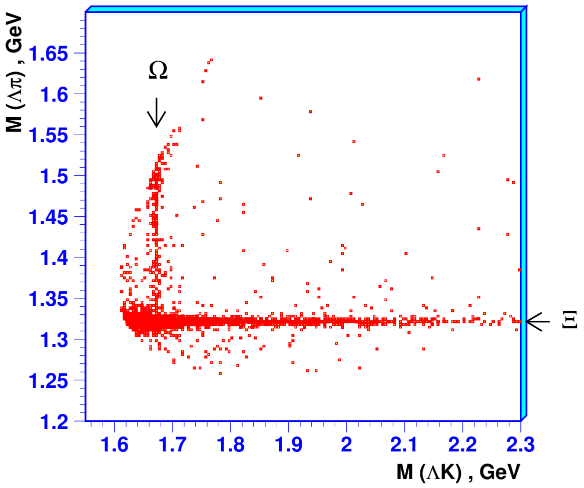

Figure 2. M($\Lambda\pi$) versus M(ΛK) for selected cascade decay candidates (Pb–Pb data sample)

Table 1 shows the data samples used for the present analysis and the expected increase in statistics after processing all collected data.

Particle	Pb–Pb		p–Pb	
	Presented	Expected	Presented	Expected
Ω^-	145	$\times 2$	15	
$\overline{\Omega}^+$	58	$\times 2$	4	
Ξ^-	1346	$\times 2$	275	
$\overline{\Xi}^+$	339	$\times 2$	101	
Λ	1868	$\times 350$	1056	$\times 100$
$\overline{\Lambda}$	669	$\times 150$	243	$\times 100$
K^0_S	750	$\times$ 1000	1100	$\times$ 200
h^-	1800	$\times 3 \cdot 10^5$	1500	$\times 5 \cdot 10^4$

Table 1. Particle statistics used in the present analysis

The data have not been corrected for feed-down. In the geometry of our experiment the feed-down for weak decays is expected to be of minor importance. It is estimated to be less than 5% for Λ and less than 10% for $\overline{\Lambda}$.

In the particle spectra the mass resolution of the peaks was better than 6 MeV (FWHM). Up to now only a fraction of the available data sample on tapes has been fully corrected for acceptance and reconstruction losses.

The acceptance windows for Ξ and Ω from Pb–Pb and p–Pb collisions are shown in Fig. 3. The corresponding acceptance windows for other analysed particles are of a similar shape. These shapes, as can be seen from the figures, are quite complicated, but due to the symmetry of Pb–Pb collisions, the reflection of data with respect to mid-rapidity (which in our case is equal to 2.91) allows us to extrapolate the particle yields to a region of one rapidity unit (centred at mid-rapidity), which is more suitable for comparison with models and other experiments.

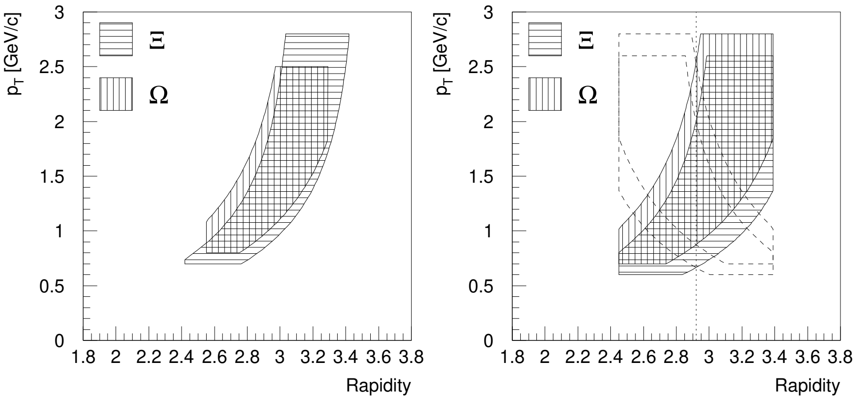

Figure 3. Acceptance windows for Ξ and Ω hyperons for p–Pb (left) and Pb–Pb (right) interactions. For Pb–Pb collisions, the symmetry of the system allows us to symmetrise the acceptance windows by reflection around y_{cm}. The reflected windows are drawn as dashed lines.

3 Transverse mass distributions

The double differential distributions for the measured particles were fitted in their respective acceptance windows using the expression

$$\frac{d^2N}{dm_{\mathrm{T}}dy} = f(y)\, {m_{\mathrm{T}}}^{\alpha} \exp(-\frac{m_{\mathrm{T}}}{T}) \tag{1}$$

where m_T is the transverse mass. The fit was performed using the maximum likelihood method.

For the present analysis, with limited statistics, we have assumed the rapidity distributions to be flat for $|y - y_{cm}| < 0.5$, *i.e.* in expression (1) $f(y)$ = constant. We have investigated the systematic error which this assumption could introduce in the case of p–Pb for h^-, K^0_S, Λ and $\overline{\Lambda}$, where published data exist for p-Au [18] and p-S [19] collisions. We find that using a flat rapidity distribution, instead of one obtained from a fit to the published data, gives a difference of $< 2\%$ on the slope and $< 10\%$ on the yield defined by equation (2) in the case of h^-, and 5% and 5% respectively in the case of the K^0_S distribution. Similarly, a flat rapidity distribution, instead of one obtained from an empirical fit to the data of [18], gives a difference of $< 5\%$ on the slope and $< 5\%$ on the extrapolated yield in the case of the $\overline{\Lambda}$ and 10% and 6% respectively in the case of the Λ distribution.

Transverse mass distributions have been fitted using expression (1), where we have chosen both $\alpha = \frac{3}{2}$ and $\alpha = 1$ [20] in order to facilitate comparisons with other experiments (*e.g.* WA85 [21], WA94 [22] and NA49 [23]). Due to the limited statistics for Ω^- and $\overline{\Omega}^+$, the combined statistics were used, both for Pb–Pb and p–Pb data. The inverse slope parameters T, resulting from the fits of m_T spectra of h^-, K^0_S, Λ, Ξ and Ω for Pb–Pb and p–Pb collisions, are summarised in table 2. Quoted errors are statistical only.

Particle	p–Pb		Pb–Pb	
	$\alpha = 3/2$	$\alpha = 1$	$\alpha = 3/2$	$\alpha = 1$
h^-	163 ± 4	185 ± 5	183 ± 6	213 ± 8
K^0_S	197 ± 5	217 ± 6	210 ± 7	232 ± 9
Λ	184 ± 5	196 ± 6	266 ± 7	289 ± 8
$\overline{\Lambda}$	172 ± 10	183 ± 11	264 ± 11	287 ± 13
Ξ^-	222 ± 12	235 ± 14	266 ± 8	286 ± 9
$\overline{\Xi}^+$	211 ± 19	224 ± 21	265 ± 15	284 ± 17
$\Omega^- + \overline{\Omega}^+$	312 ± 86	334 ± 99	238 ± 17	251 ± 19

Table 2. Inverse m_T slope parameters T in MeV for p–Pb and Pb–Pb interactions.

The inverse slope parameter T increases from p–Pb to Pb–Pb for h^-, K^0_S, Λ and Ξ. For Pb–Pb one observes very similar inverse m_T-slopes for Λ and Ξ, while a decrease in T is suggested for the heavier Ω hyperon. For p–Pb the large error on T precludes firm conclusions regarding the Ω inverse slope.

In fig. 4 the inverse slope parameters for Λ and Ξ and their antiparticles are compared with previous WA85 [21] and WA94 [22] results. As a common feature, the inverse slope parameters have similar values for proton induced reactions, while they show a clear increase with the size of the collision system for nucleus-nucleus reactions.

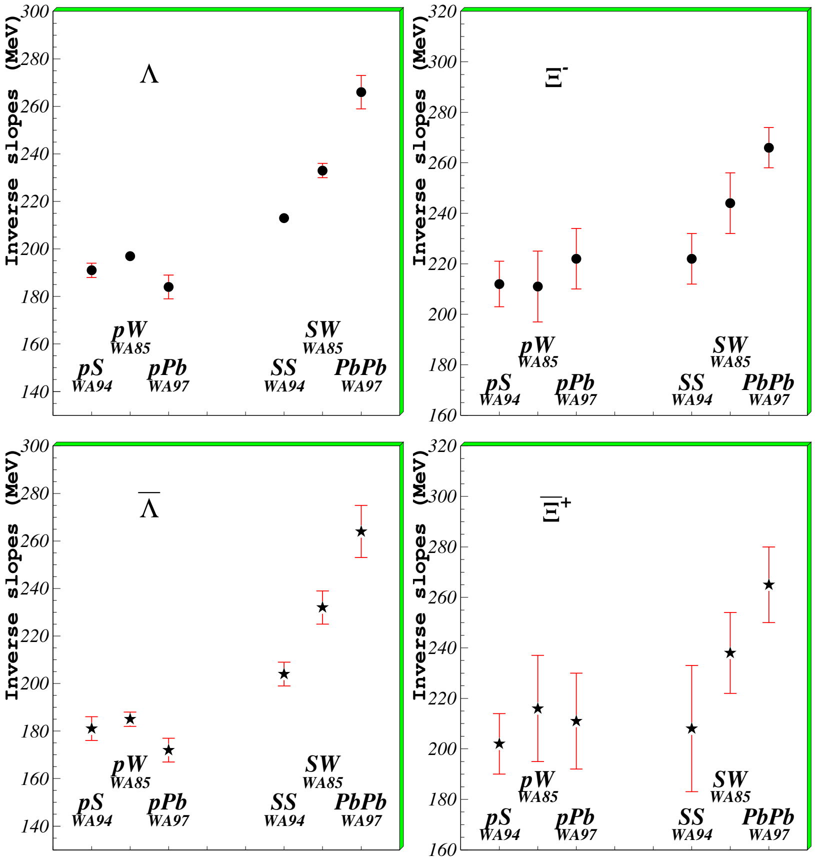

Figure 4. Inverse slopes of Λ, Ξ^-, $\overline{\Lambda}$ and $\overline{\Xi}^+$ for different colliding systems. The $\alpha = \frac{3}{2}$ value has been used.

The values of T for Pb–Pb collisions shown in table 2 and those reported by the NA49 collaboration [23] are displayed together in fig. 5 as a function of the particle mass. It appears that T increases with the mass of the particle

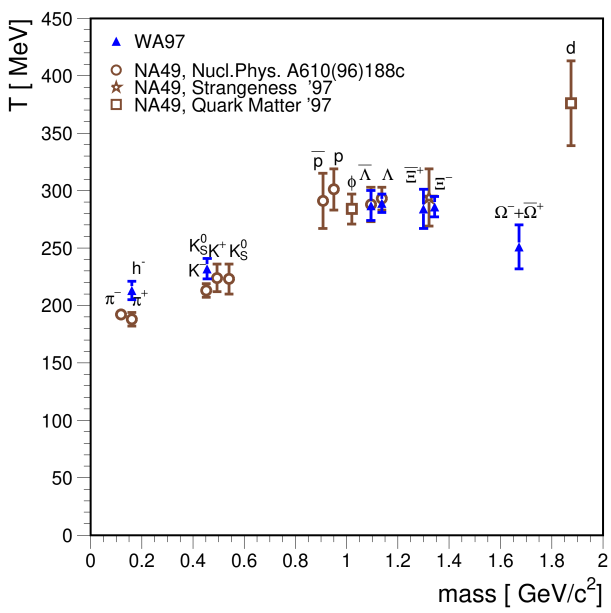

Figure 5. Inverse slope T versus particle mass.

for pions, kaons, protons and deuterons. However, this is not the case for hyperons, whose fitted inverse slope parameter T values seem to level off, with perhaps a slight decrease for Ω. A possible origin of such behaviour has been recently discussed in [24].

4 Particle yields

The particle production yield Y is defined by the integral

$$Y = \int_0^\infty \mathrm{d}p_\mathrm{T} \int_{y_{cm}-0.5}^{y_{cm}+0.5} \mathrm{d}y \, \frac{\mathrm{d}^2 N}{\mathrm{d}y \, \mathrm{d}p_\mathrm{T}} \tag{2}$$

where the extrapolation to the window $|y - y_{cm}| < 0.5$ and $p_\mathrm{T} > 0$ GeV/c is done according to expression (1).

The WA97 multiplicity detectors allow us to study hyperon production as a function of collision centrality. As a measure of the centrality, we used the number of nucleons participating in a collision N_{part}. From the multiplicity detector measurements we estimated N_{part} using a Glauber model for Pb–Pb interactions, together with the assumption of proportionality between the number of participants and the multiplicity. The method used to estimate N_{part} is described in ref. [10] and [11].

Fig. 6 shows particle yields per event for p–Pb and Pb–Pb interactions as a function of the number of participants $\langle N_{part} \rangle$. The vertical error bars correspond to statistical uncertainties only, and do not include systematic errors from feed-down nor from the assumption of a flat rapidity distribution in our acceptance window. As discussed above, these are estimated to be small relative to the current statistical errors. Horizontal bars show the root-mean-square values of the number of participants in the selected bins for Pb–Pb collisions and the full range in p–Pb.

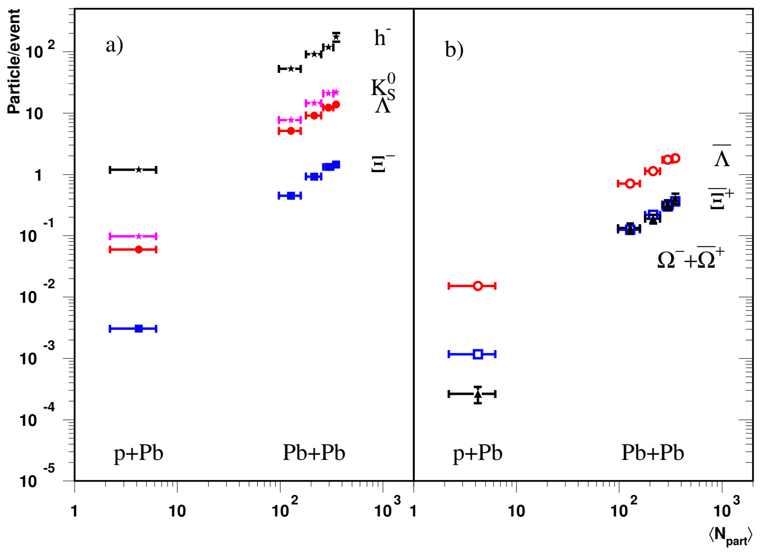

Figure 6. Yields, defined in equation (2), as a function of the number of participants for a) h^-, K^0_S, Λ and Ξ^-; b) $\overline{\Lambda}$, $\overline{\Xi}^+$ and $\Omega^- + \overline{\Omega}^+$. Note that yields for $\overline{\Xi}^+$ and $\Omega^- + \overline{\Omega}^+$ are very similar. See text for details.

In fig. 6 the particles are divided into two groups. Fig. 6a shows the particles with at least one common valence quark with the nucleon: Ξ^-, Λ, h^- and K^0_S which has both contributions $\overline{d}s$ and $d\overline{s}$. Fig. 6b refers to hyperons with no common valence quark with the nucleon: $\overline{\Lambda}$, $\overline{\Xi}^+$ and $\Omega^- + \overline{\Omega}^+$. It is instructive to analyse them separately since the particles in the two groups are empirically known to exhibit different production features, *e.g.* Λ and $\overline{\Lambda}$ have different rapidity spectra both in p-S and S-S [18].

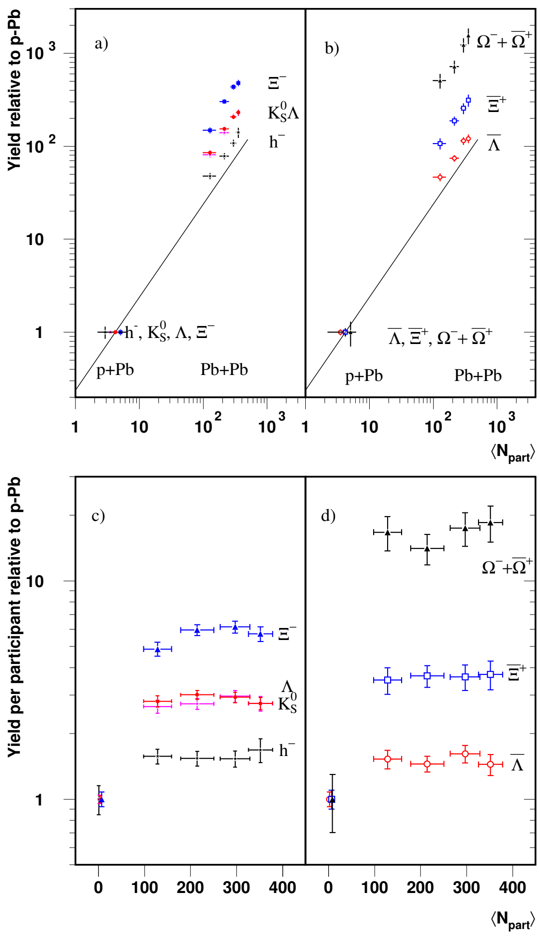

Figure 7. Yields, expressed in units of yields observed in p–Pb collisions, as a function of the number of participants for a) h^-, K^0_S, Λ and Ξ^-; b) $\overline{\Lambda}$, $\overline{\Xi}^+$ and $\Omega^- + \overline{\Omega}^+$. The solid line represent a function proportional to the number of participants $\langle N_{part} \rangle$. Yields per participant relative to p–Pb as a function of the number of participants for c) h^-, K^0_S, Λ and Ξ^-; d) $\overline{\Lambda}$, $\overline{\Xi}^+$ and $\Omega^- + \overline{\Omega}^+$. See text for details.

Fig. 7 [25] shows the particle yields expressed in units of the corresponding yield per p–Pb interaction (*i.e.* each yield is rescaled so that the value for p–Pb is set to one). It is observed that all Pb–Pb yields show a steady increase with centrality up to very central events. The particle yields in Pb–Pb are compared to a yield curve (solid line) drawn through the p–Pb points and proportional to the number of participants N_{part}.

As already pointed out in [10], the Λ, Ξ and Ω yields increase with centrality from p–Pb to Pb–Pb faster than linearly with the number of participants. At present the improved statistics allows us to study how the yields increase within our experimental centrality range for Pb–Pb, *i.e.* for $N_{part} > 100$. In this range, as shown in fig. 7, we observe that all particle yields per participant appear to be constant. This is illustrated further in fig. 7c and 7d where the strange particle yield per participant as a function of N_{part} is presented.

We use the average yield per participant $Y/\langle N_{part}\rangle$, where the yield Y, calculated using equation (2) has been integrated over the number of participants N_{part}, to compute the strangeness enhancement E going from p–Pb to Pb–Pb collisions

$$E = \left(\frac{Y}{\langle N_{part}\rangle}\right)_{Pb-Pb} \Big/ \left(\frac{Y}{\langle N_{part}\rangle}\right)_{p-Pb} \tag{3}$$

E measures the enhancement at mid-rapidity for hadron species Y. The enhancement values E for the two particle groups are displayed in fig. 8.

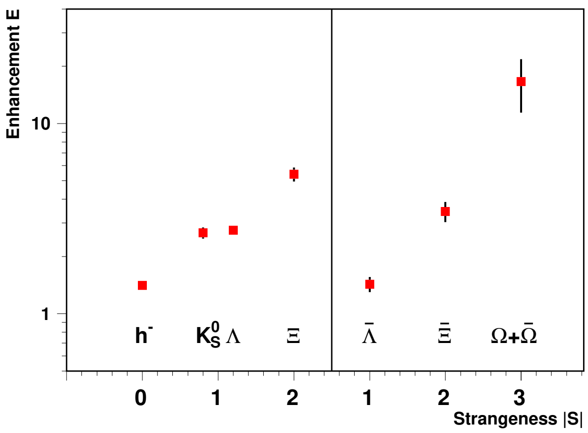

Figure 8. Strange particle enhancement versus strangeness.

Similar enhancement values are obtained if we use the data before the extrapolation to the full $y - p_{\mathrm{T}}$ window.

We note that the enhancement E increases with strangeness:

$$E(\Omega^- + \overline{\Omega}^+) > E(\overline{\Xi}^+) > E(\overline{\Lambda})$$

and, similarly, for particles with at least one quark in common with the nucleon

$$E(\Xi^-) > E(\Lambda) \approx E(\mathrm{K^0_S})$$

5 Conclusions

An analysis of the transverse mass spectra of strange particles produced in Pb–Pb and p–Pb collisions has shown that inverse slope parameters for Λ ($\overline{\Lambda}$) and Ξ^- ($\overline{\Xi}^+$) increase as a function of the size of the collision system. Comparison of our Pb–Pb data on inverse slopes with those measured by the NA49 experiment exhibits a good agreement of results for pions, kaons, Λ and Ξ. The Ω inverse slope, measured for the first time by the WA97, signalises a deviation from a linear increase of inverse slopes with the particle mass for multiply-strange hyperons.

The strange particle yields per participant increase from p–Pb to Pb–Pb at central rapidity. These enhancements are more pronounced for multistrange particles, and reach one order of magnitude in the case of Ω. However, within the participant range $N_{part} > 100$, corresponding to our Pb–Pb data, all yields are found to increase proportionally to N_{part}, thus suggesting that all the reported enhancements reach their maximum values for N_{part} below 100 and then remain constant[a].

An obvious question for future experiments, *e.g.* NA57 [28], is whether the increase in the hyperon production shown in fig. 7 is smooth with $\langle N_{part} \rangle$, or if any discontinuity is present at lower centrality values.

References

1. J. Rafelski, *Phys. Rep.* **88**, 331 (1982).
2. P. Koch, B. Müller and J. Rafelski, *Phys. Rep.* **142**, 167 (1986).
3. J.W. Harris and B. Müller, *Annu. Rev. Nucl. Part. Sci.* **46**, 71 (1996).

[a]We note that analogous behaviour has been reported for Λ and $\overline{\Lambda}$ in S–W interactions; ref. [26] reports an increase in Λ and $\overline{\Lambda}$ production relative to negatives particles at high p_T going from p–W to S–W interactions and ref. [27] shows that for central rapidity densities above 100, the Λ and $\overline{\Lambda}$ yields are proportional to the rapidity density of negative particles.

4. S.A. Bass, M. Gyulassy, H. Stöcker and W. Greiner, *Signatures of Quark-Gluon-Plasma formation in high energy heavy-ion collisions: A critical review*, hep-ph/9810281, to be published in *J. Phys. G: Nucl. Part. Phys.*
5. G.J. Odyniec, *Nucl. Phys.* A **638**, 135c (1998).
6. J.B. Kinson, in: *Proceedings of the International Conference on Strangeness in Quark Matter, Padova (Italy), July 20-24, 1998*, to be published.
7. S. Abatzis et al., *Phys. Lett.* B **393**, 210 (1997).
8. S. Abatzis et al., *Phys. Lett.* B **400**, 239 (1997).
9. I. Králik et al. (WA97 collaboration), *Nucl. Phys.* A **638**, 115c (1998).
10. E. Andersen at al., *Phys. Lett.* B **433**, 209 (1998).
11. R. Caliandro et al. (WA97 collaboration), in: *Proceedings of the International Conference on Strangeness in Quark Matter, Padova (Italy), July 20-24, 1998*, to be published.
12. R. Lietava et al. (WA97 collaboration), *ibid.*
13. A. Jacholkowski et al. (WA97 collaboration), *ibid.*
14. G. Alexeev et al., *Nucl. Phys.* A **590**, 139c (1995).
15. C. Bovet et al., *CERN Yellow Report*, CERN 82-13 (1982).
16. E.H.M. Heijne et al., *Nucl. Instrum. Methods* A **349**, 138 (1994);
F. Antinori et al., *Nucl. Instrum. Methods* A **360**, 91 (1995).
17. L. Šándor et al. (WA97 collaboration), *Nucl. Phys.* B (*Proc. Suppl.*) **71**, 270 (1999).
18. T. Alber et al., *Z. Phys.* C **64**, 195 (1994).
19. A. Bamberger et al., *Z. Phys.* C **43**, 25 (1989)
20. E. Schnedermann, J. Sollfrank and U. Heinz, *NATO ASI Series* **B303**, 175 (1993).
21. S. Abatzis et al., *Phys. Lett.* B **359**, 382 (1995).
22. S. Abatzis et al., *Phys. Lett.* B **354**, 178 (1995).
23. P.G. Jones et al., *Nucl. Phys.* A **610**, 188c (1996);
C. Bormann et al., *J. Phys.* G: *Nucl. Part. Phys.* **23**, 1817 (1997);
G. Roland et al., *Nucl. Phys.* A **638**, 91c (1998).
24. H. van Hecke, H. Sorge and N. Xu, preprint nucl-th/9804035.
25. E. Andersen et al. (WA97 collaboration), *submitted to Phys. Lett. B.*
26. J.L. Narjoux et al., *Nucl. Phys.* A **525**, 445 (1990).
27. S. Abatzis et al., *Phys. Lett.* B **244**, 130 (1990).
28. R. Caliandro et al. (NA57 Collaboration), CERN/SPSLC/96-40 SPSLC/P300, 20 August 1996.